Materials Science and Engineering C 74 (2017) 36–46

Contents lists available at ScienceDirect

Materials Science and Engineering C

journal homepage: www.elsevier.com/locate/msec

A novel hydrogel of poloxamer 407 and chitosan obtained by gamma irradiation exhibits physicochemical properties for wound management

Gerardo Leyva-Gómez [a,*], Erika Santillan-Reyes [a], E Lima [b], Abigail Madrid-Martínez [a], E Krötzsch [a], D Quintanar-Guerrero [c], David Garciadiego-Cázares [d], Alejandro Martínez-Jiménez [a], M Hernández Morales [b], Silvestre Ortega-Peña [e], ME Contreras-Figueroa [f], GE Cortina-Ramírez [g], René Fernando Abarca-Buis [a,*]

[a] Laboratory of Connective Tissue, Centro Nacional de Investigación y Atención de Quemados, Instituto Nacional de Rehabilitación Luis Guillermo Ibarra Ibarra, Mexico City, Mexico
[b] Departamento de Materiales Metálicos y Cerámicos, Instituto de Investigaciones en Materiales, Universidad Nacional Autónoma de México, Mexico City, Mexico
[c] Laboratorio de Investigación y Posgrado en Tecnología Farmacéutica, Facultad de Estudios Superiores Cuautitlán, Universidad Nacional Autónoma de México, State of Mexico, Mexico
[d] Unidad de Ingeniería de Tejidos y Medicina Regenerativa, Instituto Nacional de Rehabilitación Luis Guillermo Ibarra Ibarra, Mexico City, Mexico
[e] Laboratorio de Infectología, Instituto Nacional de Rehabilitación Luis Guillermo Ibarra Ibarra, Mexico City, Mexico
[f] Bioterio y Cirugía Experimental, Instituto Nacional de Rehabilitación Luis Guillermo Ibarra Ibarra, Mexico City, Mexico
[g] Departamento de Biología, Instituto Nacional de Investigaciones Nucleares, Mexico City, Mexico

ARTICLE INFO

Article history:
Received 19 September 2016
Received in revised form 7 December 2016
Accepted 16 December 2016
Available online 7 January 2017

Keywords:
Polymer
Skin
Wound repair
Crosslinking
Cobalt-60

ABSTRACT

Application of polymers cross-linked by gamma irradiation on cutaneous wounds has resulted in the improvement of healing. Chitosan (CH) and poloxamer 407 (P407)-based hydrogels confer different advantages in wound management. To combine the properties of both compounds, a gamma-irradiated mixture of 0.75/25% (w/w) CH and P407, respectively, was obtained (CH-P), and several physical, chemical, and biological analyses were performed. Notably, gamma radiation induced changes in the mixture's thermal behavior, viscosity, and swelling, and exhibited stability at neutral pH. The thermal reversibility provided by P407 and the bacteriostatic effect of CH were maintained. Mice full-thickness wounds treated with CH-P diminished the wound area during the first days. Consequently, with this treatment, increased levels of macrophages, α-SMA, and collagen deposition in wounds were observed, indicating a more mature scar tissue. In conclusion, the new hydrogel CH-P, at physiologic pH, combined the beneficial characteristics of both polymers and produced new properties for wound management.

1. Introduction

Hydrogels for wound healing are materials that protect injuries, avoiding and/or controlling infection, and providing moisture for the irregular wound environment. These materials are prepared from different natural and synthetic polymers, and are employed individually or as mixtures. Some polymers, such as chitosan (CH) and poloxamer 407 (P407), have demonstrated healing properties. In this respect, CH is a linear polysaccharide derived from chitin, and CH hydrogels are prepared by dissolution of CH in aqueous acidic solution. Depending on the degree of deacetylation, CH is biodegradable, biocompatible, and can be manufactured in different shapes [1]. Due to its positive chemical charges at physiological pH, CH presents bioadhesive properties. During wound healing, CH hydrogels allow cell adhesion and stimulate proliferation and cell differentiation [2–4]. On the other hand, P407 is a synthetic polymer that possesses the property of thermo-reversibility, which modulates gelation upon temperature change. This feature permits biomedical applications, employing the change from ambient-to-physiological temperature to release drugs in various administration vias [5–6]. Hydrogels prepared with P407 have been employed to improve wound repair; when administered during 14 days in full-thickness excisional wounds performed in the dorsal skin of rats, P407 promoted an increase of wound contraction and closure at days 11 and 14 post-wounding. Meanwhile, the increase in Vascular Endothelial Growth Factor (VEGF) and Transforming Growth Factor (TGF)-β1 level expression was observed on days 3 and 7 post-wounding, respectively, and simultaneously with leukocyte infiltration, fibroblast proliferation, and marked angiogenesis; improving granulation tissue formation [7].

* Corresponding authors at: Laboratory of Connective Tissue, Centro Nacional de Investigación y Atención de Quemados, Instituto Nacional de Rehabilitación Luis Guillermo Ibarra Ibarra, Calz. México-Xochimilco No. 289, Col. Arenal de Guadalupe, Del. Tlalpan, C.P. 14389 Mexico City, Mexico.
E-mail addresses: gerardoleyva@hotmail.com (G. Leyva-Gómez), kikita5410@gmail.com (E. Santillan-Reyes), lima@iim.unam.mx (E. Lima), abitzy@hotmail.com (A. Madrid-Martínez), kroted@yahoo.com.mx (E. Krötzsch), quintana@unam.mx (D. Quintanar-Guerrero), dagarcaz@yahoo.com (D. Garciadiego-Cázares), escarubi@gmail.com (A. Martínez-Jiménez), magic140288@hotmail.com (M. Hernández Morales), silvestreortega@yahoo.com.mx (S. Ortega-Peña), elenacnr@yahoo.com.mx (M.E. Contreras-Figueroa), gloriaemeli.cortina@inin.gob.mx (G.E. Cortina-Ramírez), buisr@yahoo.com (R.F. Abarca-Buis).

http://dx.doi.org/10.1016/j.msec.2016.12.127
0928-4931/

In general, a combination of polymers to prepare hydrogels can be obtained by physical (freeze-thawing), and by chemical or high-energy radiation methods [8]. The latter is considered a suitable tool for cross-linking polymers because it is simple, faster, clean, effective, and economically and environmentally friendly. It does not require chemical catalysts, toxic chemicals, extreme physical conditions, initiators, or cross-linkers, and conducting two processes (crosslinking and sterilization) at the same time is possible [8], offering an alternative technique to conventional methods for developing novel polymeric products [9]. Previously, our investigation group developed a new collagen-polyvinylpyrrolidone copolymer by gamma irradiation that is characterized by immunomodulatory, fibrolytic, and antifibrotic properties, demonstrating the advantages of modification of polymers by high-energy radiation methods [10]. Some background on the benefits of gamma irradiation in obtaining materials with potential use in wound healing includes the combination of *O*-carboxymethyl CH/gelatin [11], poly(vinyl alcohol) (PVA)/sodium alginate [12], PVA/hydroxyethyl starch [13], PVA/CH [14] PVA/CH-glycerol [15], PVA/polyvinylpyrrolidone (PVP) [16] and PVA/polyethylene glycol (PEG) [17], among others [18]. However, few of these studies developed the physicochemical characterization and evaluation of wound healing in an *in vivo* model. The aim of this work was to assess the wound healing properties of a new hydrogel prepared from a physical mixture of CH and P407, cross-linked by gamma irradiation (CH-P). This hydrogel maintained the thermo-reversibility of P407, although the thixotropy was absent. In addition, the novel compound presented stability at neutral pH, swelling ability in contact with blood serum, and an antimicrobial/antifungal effect, and promoted the wound healing in a model of excisional wounds carried out on mice. These features rendered the hydrogel suitable for wound management.

2. Materials and methods

2.1. Materials

Low-molecular-weight CH (75–85% deacetylated, batch number: SLBJ5775V (20–300 cP, 1 wt.% in 1% acetic acid, according to the manufacturer's specifications), was purchased from Aldrich Chemistry (Iceland). Pluronic® F-127 (poloxamer 407, P407, $HO(C_2H_4O)_{101}(C_3H_6O)_{56}(C_2H_4O)_{101}H$, CMC: 950–1000 ppm [~25 °C], lot number: SLBL1780V) was acquired from Sigma Life Science (MO, USA). The antibodies anti-elastase (ab21595), anti-F4/80 (ab6640), anti-α smooth muscle actin (α-SMA) (ab7817), and anti-TGF-β3 (ab15537) were purchased from Abcam (MA, USA). Goat anti-rabbit Texas Red (W0901) was obtained from Vector Laboratories (CA, USA); goat anti-rat IgG-FITC (SC-2011) was acquired from Santa Cruz Biotechnology (CA, USA), and goat anti-mouse IgG-Alexa Fluor® 488 was purchased from Molecular Probes (IL, USA). The immunofluorescence reactions were mounted with Vectashield®/DAPI, from Vector Laboratories. All other solvents and chemicals were of analytical grade.

2.2. Sample preparation

2.2.1. CH solution (CH)

A solution of 0.75% (w/w) of CH was prepared in 0.5% acetic acid in water. Subsequently, this was maintained under stirring at room temperature during 24 h. Afterward, the suspension was filtered.

2.2.2. Hydrogel of P407

A 25% solution (w/w) of P407 in ultrapure water was prepared by stirring the polymer during 5 h at 4 °C. The final solution was filtered at the same temperature.

2.2.3. Hydrogel of the CH and P407 mixture (CH+P)

A solution of 0.75/25% (w/w) of CH and P407, respectively, was prepared in 0.5% acetic acid in water at 4 °C. Subsequently, this was maintained under stirring at the same temperature during 24 h. Then, the suspension was filtered.

2.2.4. Gamma-irradiated hydrogel (CH-P)

The CH+P solution, prepared as previously noted, was subjected to gamma radiation (^{60}Co) at an absorption-rate of 25 kGy in a Transelektro LGI-01, IZOTOP Institute of Isotopes Co. (Budapest, Hungary), with 3247.01 Ci and a dose ratio of 0.249 kGy/h (Instituto Nacional de Investigaciones Nucleares). Due to the nature of the formula, the final pH was 4.6 (CH-P 4). This property, although unphysiologic, was considered useful for evaluating the CH-P hydrogel during wound healing, because the acidic condition could control microorganism development. However, considering the biological condition of wounds, neutral pH is desirable for maintaining homeostasis. In order to obtain a hydrogel with neutral pH, CH-P 4 was adjusted to pH = 7 by the addition of triethanolamine (CH-P 7).

2.3. Sample characterization

2.3.1. Fourier Transform Infrared Spectroscopy (FTIR)

The chemical structure was investigated using FTIR spectroscopy with a Bruker Alpha platinum spectrometer (MA, USA), within the 4000–400 cm^{-1} range, with a resolution of 4 cm^{-1} and an average of 32 scans. The analysis was performed in triplicate.

2.3.2. Nuclear Magnetic Resonance (NMR)

Proton Nuclear Magnetic Resonance (^1H NMR) measurements were performed using a Bruker Advance 400 Spectrometer (MA, USA) (static field = 9.4 T) operating at a frequency of 100.61 MHz at 25 °C. Samples were dissolved in deuterated water (D_2O). The spectra were processed employing TOP Spin software. Each evaluation was performed in triplicate.

2.3.3. Morphological analysis

Scanning Electron Microscopy (SEM) was performed in each freeze-dried formula by means of a JEOL 6000 microscope (MA, USA) operated at an accelerating voltage of 20 kV. The sample was mounted on a conductive carbon tape. Each evaluation was performed in triplicate.

2.3.4. Thermal analysis

Thermal characterization of the hydrogels previously lyophilized, was performed by Differential Scanning Calorimetry (DSC) employing DSC Q100 (TA) (DE, USA) equipment, previously calibrated with an indium sample and baseline with an unsealed aluminum sample holder. A total of 3 mg of powder was analyzed in a range of 0–200 °C with a heating rate of 10 °C/min, employing nitrogen to purge the gas chamber. The analysis was performed in triplicate.

2.3.5. Viscosity profiles of hydrogels

The variation of viscosity with an increasing agitation speed and its recovery was carried out utilizing a viscosity-recording method with a Brookfield CAP 2000 viscosimeter (MA, USA) at 37 °C. The equipment was previously calibrated with standard number 30,000 for the use of a no. 3 needle. A 100-μL volume of each hydrogel was placed into the equipment and viscosity was recorded within a range of 120–600 rpm in forward and in reverse order at 20-rpm intervals. The analysis was performed in triplicate.

2.3.6. Time and temperature of gelation

Sol-gel transition of hydrogels (P407, CH+P, CH-P 4, and CH-P 7) was carried out employing the same equipment and conditions as those for viscosity profiles. The transition point was defined by the temperature and time when the viscosity increased sharply [19]. A 100-μL volume of each hydrogel was placed into the equipment, and a viscosity within the range of 7–30 °C with a change speed of 1 °C/10 s at 50 rpm was recorded. An acrylic chamber with a cotton bed dampened with

water, to maintain constant relative humidity, was employed. The analysis was performed in triplicate.

2.4. Sample evaluation

2.4.1. The hydrogel's ability to regulate different relative humidities

With the aim of determining the capacity of the hydrogel to regulate moisture in the environment, different solutions of glycerol/water were prepared to establish different relative humidities, and the uptake or removal of water was determined by a gravimetric method. This analysis of hydrogels was performed in semi-solid state, as they were applied in the in vivo model. A total of 5 mL of each hydrogel was placed in a 10 mL-vessel; these were left to rest for 12 h at room temperature and were then placed in a chamber with different relative humidities. In detail, solutions of 92, 89, 84, 79, 72, 64, 51, and 33% *w*/*v* of glycerol in water yielded the following relative humidities: 20, 30, 40, 50, 60, 70, 80, and 90%, respectively. Later, the system was placed in a 37 °C oven for 6 h, and the device was then weighed. The % of absorbed or eliminated water was determined by weight difference. Each evaluation was performed in triplicate.

2.4.2. Bioerosion/swelling test

In order to predict a hydrogel's behavior when in contact with a wound, a bioerosion/swelling assay of the different formulas was performed in vitro. The assay was determined by a gravimetric method. In the same manner, this analysis of hydrogels was performed in semi-solid state, as they were applied in the *in vivo* model. A total of 1 mL of each hydrogel was placed at the bottom of glass tubes (25 mL) at 4 °C. Subsequently, the hydrogels were maintained at room temperature for 12 h, and then human blood serum obtained from the Blood Bank of the National Rehabilitation Institute, Mexico City, Mexico, was added. Tubes were placed in a BS-06 (Lab Companion, Kyunggi-Do, South Korea) water bath at 37 °C with constant stirring at 50 rpm. After 2, 4, 6, 8, 10, 12, 15, 18, 21, and 24 h, supernatants were removed by decantation. Degree of swelling or bioerosion was determined by the weight difference of the residues. This test was performed in triplicate.

2.4.3. Evaluation of the antimicrobial activity of the polymers

The antimicrobial activity of each formula was evaluated through a contact method [20–21] against Gram-negative bacteria (*Escherichia coli*, ATCC25922 and *Pseudomonas aeruginosa*, clinically isolated), Gram-positive bacteria (*Staphylococcus aureus*, ATCC 25923), and fungi (*Candida albicans*, clinically isolated). Suspensions of each microorganism were prepared with 0.5 MacFarland standards (1.5×10^8 colony-forming units/mL), and 200 μL of the suspension was deposited and spread on Müeller-Hinton agar plates. Previously, sterile filter-paper discs (6 mm in diameter) were impregnated with 25 μL of each formula at 5 °C, and the discs were then placed onto the inoculated agar plates and incubated for 24 h at 37 °C. Finally, the inhibition halos were measured. Evaluation was performed in triplicate and, as negative control, filter-paper discs with 25 μL of sterile distilled water were used.

2.4.4. In vivo evaluation in an excisional full-thickness wound model

This study was carried out in accordance with the Guide for the Care and Use of Laboratory Animals of Mexican Official Norm NOM-062-ZOO-1999 and the study approved by the Internal Committee for the Care and Use of Laboratory Animals of the Instituto Nacional de Rehabilitación, Mexico. Two month-old CD1 stock male mice were utilized in this study. Animals were anesthetized with an intraperitoneal injection of Ketamin (100 mg/kg) and Xylazine (10 mg/kg). The backs of the mice were shaved and two circular excisional wounds, 5 mm in diameter each, were excised employing a biopsy punch. The wounds were washed with PBS. Afterward, 100 μL of Phosphate-Buffered Saline (PBS) solution, CH, P407, P407+CH, CH-P 4, or CH-P 7 was applied daily until wound samples were obtained; animal triplicates were evaluated. Wounds were collected and fixed at 3, 7, and 11 days post-wound (dpw). Wound photographs were captured daily using a stereo microscope (Discovery, V20; Carl Zeiss, Gottingen, Germany) and an AxioCam HRc Digital Camera (Carl Zeiss, Gottingen, Germany). The wounded area was measured utilizing AxioVision LE software (Carl Zeiss, Gottingen, Germany). Subsequently, the wounds were paraffin-embedded and serial, 5-μm-thick tissue sections were obtained.

2.4.5. Histomorphological evaluation of wounded tissues

Herovici staining to reveal collagen content and immunofluorescence to detect neutrophil elastase, F4/80, α-SMA, and TGFβ3 was performed. Anti-neutrophil elastase (1:200), anti-F4/80 (1:100), anti-α-SMA (1:50), and anti-TGFβ3 (1:50) antibodies were diluted and utilized in a 1% albumin solution. Goat anti-rabbit IgG-Texas Red (1:1000) was employed as a secondary antibody to detect anti-neutrophil elastase and anti TGFβ3. Goat anti-rat IgG-FITC (1:50) and goat anti-mouse IgG-Alexa Fluor® 488 (1:1000) were utilized as secondary antibodies to detect anti-F4/80 and anti-α-SMA, respectively.

3. Results and discussion

The results of this study show that gamma irradiation can be used to modify polymers and to obtain new properties that can be utilized in the medical field. The effects of 25 kGy gamma radiation modified the structure and properties of CH, P407 and their mixture, suitable for improving excisional wound healing by means of a process to obtain polymers that is fast, easy, and inexpensive. The new polymer was more stable due to gamma irradiation in terms of solubility at different pH, and a variation in pH, precipitation, color, viscosity, thermoreversibility, growth of bacteria/fungi, and *in vivo* activity over time was not observed. Also, modifications regarding variation between batches, and the person who prepared each batch were not observed. Additionally, the cross-linking process produces a sterile material.

3.1. Sample characterization

3.1.1. Hydrogel neutralization assay

With the aim of providing a non-irritating gel for application on wounds and, due to the fact that CH is soluble only in acidic solutions [22], hydrogel pH was neutralized. This condition was only reached when triethanolamine was added to CH-P 4. This effect can be explained by the formation of complexes comprised of units of *N*-acetyl-glucosamine with P407 chains by means of micelles, favoring its solubility in a broad pH range [23] undisturbed in the wound. This modification increases the number of medical applications that can be performed with CH products.

3.1.2. Analysis of ATR-FTIR spectra

ATR-FTIR spectra of samples are depicted in Fig. 1A. The P407 spectrum exhibits the absorption band at 2880 cm^{-1}, which is due to the stretching mode of C—H bonds, while the band due to stretching of C—O was observed at 1090 cm^{-1}. Through the CH spectrum, it can be observed that the characteristic absorption bands of functional groups appear at 1532 cm^{-1} (—NH_2 bending) and 1372 cm^{-1}, assigned to the vibration of C—H. Another broad band, ranging from 3600 to 2800 cm^{-1}, is due to amine N—H and hydroxyl O—H stretching vibrations. The band near 1150 cm^{-1} corresponds to the saccharide structure of CH, while the broad band at 1040 is assigned to C—O stretching vibration.

The CH+P spectrum practically matches that of P407, indicating that no interaction is promoted with this combination and that it is in line with P407 being the major component in this mixture. The most noticeable result is observed in the spectra of the gamma-irradiated samples. In both samples (CH-P 4 and CH-P 7), their spectra generally fit that of P407, but normalized intensities reveal a subtle increase in intensity of the C—H band. For instance, intensity ratios (measured by OMNIC software) of bands at 2880 and 1090 cm^{-1} is 1.13, 1.19, and 1.20 for CH+P,

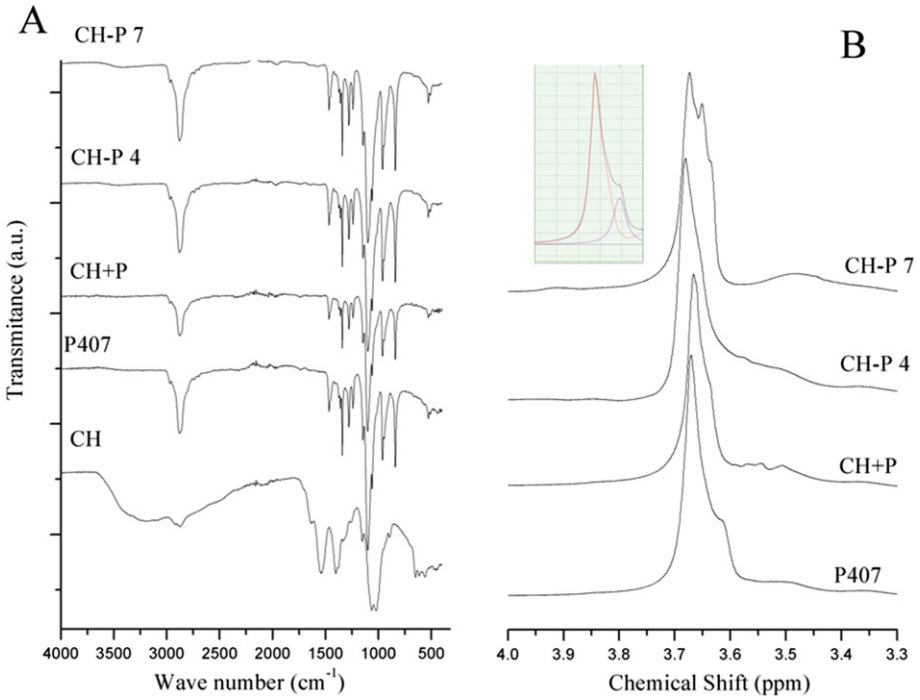

Fig. 1. ATR-FTIR (A) and ^{1}H NMR (B) spectra of CH, P407, CH+P, and copolymers CH-P 4 and CH-P 7. Inset in Panel B corresponds to deconvolution of ^{1}H NMR spectrum of P407 performed using MestReNova software.

CH-P 4, and CH-P 7, respectively. Note that P407 is a poly(ethylene oxide)/poly(propylene oxide)/poly(ethylene oxide) (PEO/PPO/PEO) triblock copolymer. Thus, it is suggested that a cross-linking between two polymers could occur in a such a way that more (PEO)(PPO)(PEO) chains are present.

3.1.3. Analysis of ^{1}H NMR spectra

^{1}H NMR spectra (Fig. 1B) are useful to evidence the different chemical environments of CH-P samples; thus, they are complementary and in line with FTIR results (Fig. 1A). In the spectrum of the P407 sample, two signals were observed: a peak is resolved at 3.67 ppm and a shoulder-peak, at 3.61 ppm. Both signals were assigned to CH_2 groups deriving from PEO and PPO units, respectively. Therefore, the ratio of the intensities of these two NMR signals is proportional to the ratio of PEO/PPO units. From this approach, it is clear that in CH+P, the ratio of PEO/PPO units is near that of P407. The spectra of gamma-irradiated samples present an evolution in this ratio. Clearly, the intensity of groups associated to PPO units increases with irradiation, which is plainly observed in the spectrum of the CH-P 7 sample. This result is in line with FTIR results. Even when two techniques suggest a cross-linking of CH_2 with P407, it is difficult to conclude indisputably concerning the mechanism employed to achieve this. NMR results are clear, showing evolution of (CH_2—CH_2—O) units, and one possibility of this happening is that cross-linking occurs between these units and the oxygen bonds, bridging the units and the glucosamine units (Fig. 2).

3.1.4. Determination of morphology by SEM

Sample morphology was assessed by SEM (Fig. 3) with the aim of identifying alterations in the materials due to gamma radiation. CH revealed a characteristic fibrous network, while P407 exhibited an amorphous structure and CH+P demonstrated a dough-like pattern by means of the penetration of the amorphous structure in the fibrous network. However, CH-P 4 and CH-P 7 structural arrangements were closer to P407 structure than CH+P, in which CH-P 7 particle size was lower than that of CH-P 4, both decreases due to the fragmentation of gamma radiation. Thereby, despite that this analysis is from lyophilized samples, a modification in physical appearance was confirmed as a result of a chemical change.

3.1.5. Obtention of thermal behavior by DSC

The characteristic properties of individual materials and possible modifications by gamma irradiation on the thermal behavior of lyophilized material are depicted in Table 1 as melting points. In this respect, CH+P produced a decrease in the thermal-event peak, indicating an interaction between the two materials. A predominance of P407 values (thermal transition and enthalpy) was observed, due to the greater mass ratio. Gamma radiation resulted in a decrease of the thermal event compared with CH+P, and a modification is also observed due to pH 7 adjustments (by the addition of triethanolamine). These observed changes suggest a slight modification of the structure due to gamma radiation.

3.1.6. Determination of viscosity profiles, time, and temperature of gelation by rheology

The viscosity profiles of different samples-of-interest are illustrated in Fig. 4. Poloxamer 407 possesses a thixotropic character due to the separation in the relaxation-recovery profile. The addition of CH to P407 (CH+P in Fig. 4) decreased viscosity, possibly by decreasing interchain forces, but increased the thixotropic characteristics. Interestingly, when the mixture of both polymers was subjected to gamma radiation (CH-P 4 in graph), magnitude-of-viscosity was increased and thixotropy was absent. Generally, by high-energy radiation, an excision of the polymer chains can be observed, thus a decrease in molecular weight and viscosity, while in the other, there is no effect on viscosity with an exposure-dose. In this study, the increase in viscosity can be caused by an increase in molecular weight due to depolymerization (principally P407, due to the greater mass ratio) and crosslinking (CH+P) via formation of covalent bonds, intermolecular interactions via Van der Waals, and H bonds favoring the organization of geometries with nuclei hydrophobic and quick self-organization when subjected to shear forces and, for this reason, also the absence of thixotropy. In addition, according to the suggested structure for the crosslinked polymer and the data of FTIR and ^{1}H NMR, it could be that an additional effect of branching,

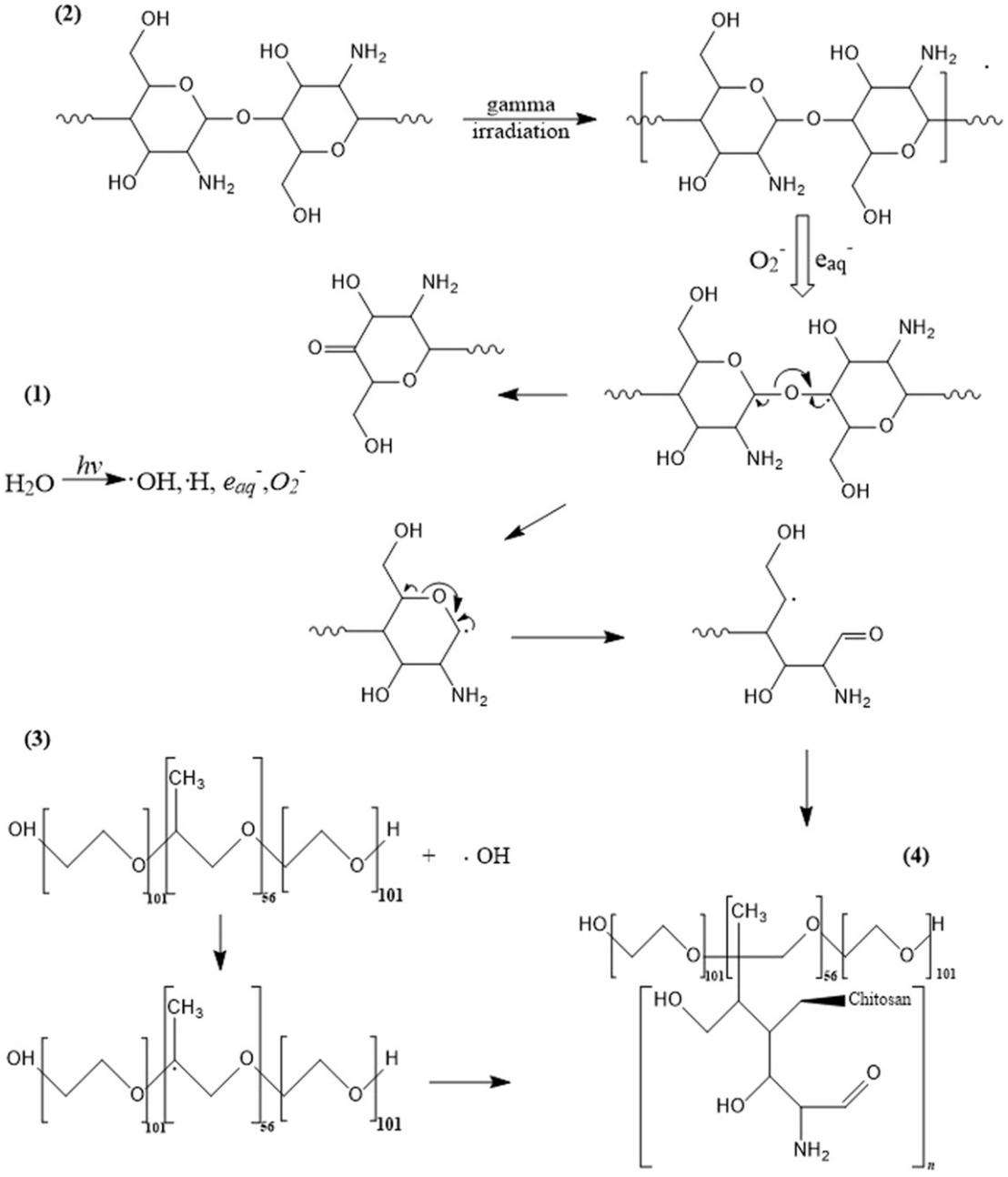

Fig. 2. The suggested cross-linking process of the chitosan (CH)-poloxamer 407 (P407) polymer under gamma irradiation. Radiolysis species of water (1) produced fragmentation of the CH chain into D-glucosamine units (2) and induced the graft on the PPO block (3) of P407 (4). P407 appeared as a low radiosensitivity polymer [24]. Additional information may be required to confirm this hypothesis.

decreased flexibility, tangled chain, and increase in friction produced a higher viscosity. Particularly, for CH-P 7, the absence of thixotropy is completely evident. These results indicate that gamma irradiation exerts an effect on the structure of materials.

Related with the previously presented data, gelation time and temperature were recorded by viscosity changes (Table 1). All hydrogels demonstrated gelation [5], except CH. The addition of CH to P407 decreased gelation time and temperature, while gamma radiation produced an increase in both parameters with respect to P407. It is noteworthy that, even with the structural changes produced by gamma radiation, P407 chains maintained their ability of thermo-reversibility. However, when pH was adjusted to neutral after irradiation (CH-P 7), there was no difference regarding P407 in both parameters (temperature and time). Conservation of thermo-reversibility in very similar terms to P407 is beneficial for wound healing because the same possibilities for application remain for P407; for example, application under cold conditions to cover the lesion area for rapid application, greater extension, penetration, and gelation on the wound once it reaches body temperature and, in addition as drug controlled-release reservoirs once gelified above or within the wound.

3.2. Sample evaluation

3.2.1. Determination of the hydrogel's ability to regulate different relative humidities

With respect to moisture management in wounds, because injuries can acquire different degrees of moisture, thus delaying or accelerating wound healing, [25–27] a hydrogel must possess the ability to provide the lesion with humidity, capturing excessive exudate while providing water for the application site in order to prevent desiccation [28], in

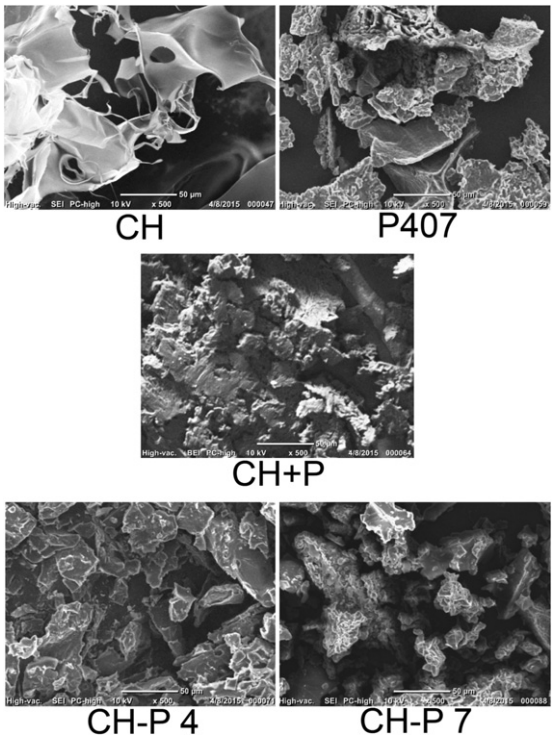

Fig. 3. Gamma radiation produces a change in the morphology of the lyophilized powders. Photomicrographs obtained by Scanning Electron Microscopy (SEM) of the lyophilized samples observed with a zoom of 500× (scale bar is equivalent to 50 μm).

order to allow cell migration across the wound surface, granulation, and re-epithelialization. Moist wound treatment avoids scab formation and increases wound closure, allowing the formation of a layer of cells on the wound's surface that closes it from the top [29]. The water-transfer rate during 6 h from hydrogels to environments with diverse relative humidities is depicted in Fig. 5A. There is a linear and inverse relationship between water transfers from hydrogels toward environments with different relative humidities. This means that the tested hydrogels can transfer a certain amount of moisture according to the wound type, for example, in the case of wounds with scarce exudate, hydrogels could promote moistening for at least 6 h. There is no variation among samples-of-interest.

3.2.2. Determination of bioerosion/swelling

Because we observed both a bioerosion and swelling effect (Fig. 5B), we can explain both characteristics as follows: the types of interaction of hydrogels with human serum can be related with viscosity, intermolecular forces and pore size. In the evaluated materials, we observed that when the viscosity is low, a bioerosion effect predominated (P407, CH+P), and between these, when intermolecular forces (CH+P) decreased, bioerosion increases. The addition of CH to P407 decreased intermolecular attraction by intercalation among P407 chains and increased the formation of hydrogen bonds with water molecules; thus, a higher capacity of bioerosion was observed. Moreover, with respect to pore size, if we take the SEM photographs as reference, we can assume that CH could confer a larger pore size on P407 in the CH+P mixture compared with the P407 hydrogel; however, in combination with the first two variables, the final effect is bioerosion. Regarding the irradiated polymers (CH-P), we observed an increase in viscosity, which could delay the entry of the human serum into the hydrogel, and we also assumed an increase in intermolecular forces due to interpenetrated networks by covalent bonds compared with CH+P, this produces a swelling effect. In addition, if we take the observed SEM particle size as reference, it would appear that the pores formed by CH-P4 and CH-P 7 do not differ with respect to CH+P. Among CH-P 4 and CH-P 7 polymers, it may be that the pore size increases in CH-P 7 due to an increase in pH; hence its swelling capacity. The characteristic swelling should allow for absorption of the wound exudate in order to promote fibroblasts migration and extracellular matrix turnover; the effect of gamma radiation allows new materials (CH-P 4 and CH-P 7) to possess that ability. Differences between CH-P 4 and CH-P 7 were observed only during the last 6 h. The gamma irradiation effect on hydrogel performance was again demonstrated through this evaluation.

3.2.3. Determination of the antimicrobial effect

It has been demonstrated in other studies, that protonated amino groups in CH provide a bacteriostatic effect against a broad range of bacteria [30] and fungi [31]. This activity depends on CH molecular weight in an inversely proportional manner, and the deacetylation degree. The polycationic nature of CH interacts with the surface of bacterial cells (interaction between CH cationic groups and anionic groups on the surface of bacterial cells, producing bacteria flocculate) and alters membrane permeability, producing an osmotic imbalance and inhibiting the transport of essential nutrients. Additionally, the interaction of these positively charged groups with DNA and RNA inhibits fungal and bacterial protein synthesis [32]. The question on whether hydrogel changes generated by gamma irradiation affect CH bacteriostatic and fungistatic properties derives from the hypothesis that gamma radiation produces various chemical changes including fragmentation, in which it could be possible that CH reduces its molecular weight and increases its bacteriostatic effect. Otherwise, the cross-linking derived from gamma irradiation could block protonated amino groups and diminish antiseptic effects. It is widely known that P407 had no microbicidal effect, while CH did. Specifically, differences in bacteriostasis were observed when CH and P407 were mixed, as well as when they were irradiated. Although not statistical differences were observed between the hydrogels with CH, slightly changes were observed in clinical isolates, specimens representing greater interest from a clinical viewpoint due to their high bacterial drug resistance. In this manner, when *Pseudomonas aeruginosa* cultures were treated with CH-P 7, an increase of growth inhibition was observed. Interestingly, this specific formula exerted no effect

Table 1
The gamma radiation produces changes in the thermal parameters; however, gelation of the new hydrogels is similar to P407. Thermal parameters obtained from differential scanning calorimetry, and time and temperature gelation values obtained by the method of viscosity, in which data are presented as mean ± Standard Error of the Mean (S.E.M.).

Hydrogel	Thermal behavior		Gelation	
	Thermal transition (°C)	Enthalpy (J/g)	Temperature (°C)	Time (s)
CH	100.79 ± 9.49	225.90 ± 34.68	–	–
P407	55.40 ± 0.50	116.30 ± 10.81	12.75 ± 0.00	92.62 ± 9.87
CH+P	54.78 ± 0.12	118.74 ± 3.91	9.47 ± 0.28[a]	65.90 ± 1.62[f]
CH-P 4	53.06 ± 0.55	106.03 ± 11.78	13.50 ± 0.26[b,c]	118.71 ± 11.72[g,h]
CH-P 7	49.92 ± 0.57	93.92 ± 2.21	12.02 ± 0.55[d,e]	93.13 ± 6.79[i,j]

One-way Analysis of Variance (ANOVA), followed by Scheffe's F test for gelation temperature: [a]CH+P vs. P407, $p < 0.0001$; [b]CH-P 4 vs. P407, $p = 0.0075$; [c]CH-P 4 vs. CH+P, $p < 0.0001$; [d]CH-P 7 vs. CH+P, $p = 0.0020$ and [e]CH-P 7 vs. CH-P 4, $p = 0.0130$. One-way Analysis of Variance (ANOVA), followed by Scheffe's F test for gelation time: [f]CH+P vs. P407, $p = 0.0098$; [g]CH-P 4 vs. P407, $p = 0.0419$; [h]CH-P 4 vs. CH+P, $p = 0.0015$; [i]CH-P 7 vs. CH+P, $p = 0.0025$ and [j]CH-P 7 vs. CH-P 4, $p = 0.0307$.

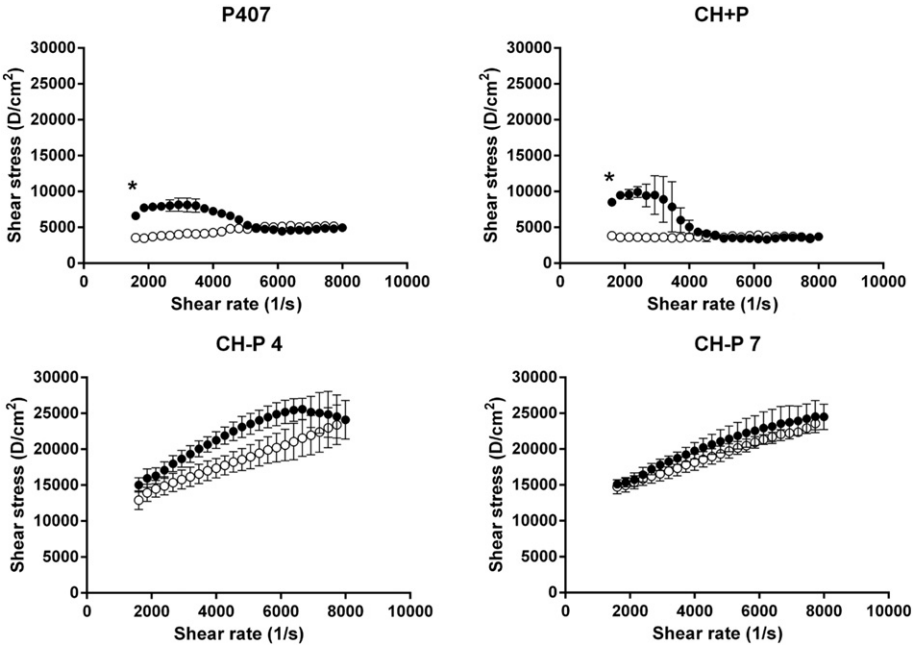

Fig. 4. The addition of CH to P407 increases viscosity, while gamma radiation produces the absence of thixotropy with an increase in viscosity. Viscosity profiles obtained employing a viscometer. Data are presented as mean ± Standard Error of the Mean (S.E.M.) and forward and reverse speed, filled and empty circles, respectively. *Significant differences with the statistical paired Student *t*-test: P407 (1600 s^{-1}, $p = 0.0036$; 4799 s^{-1}, $p = 0.0027$) and CH + P (1600 s^{-1}, $p = 0.0003$).

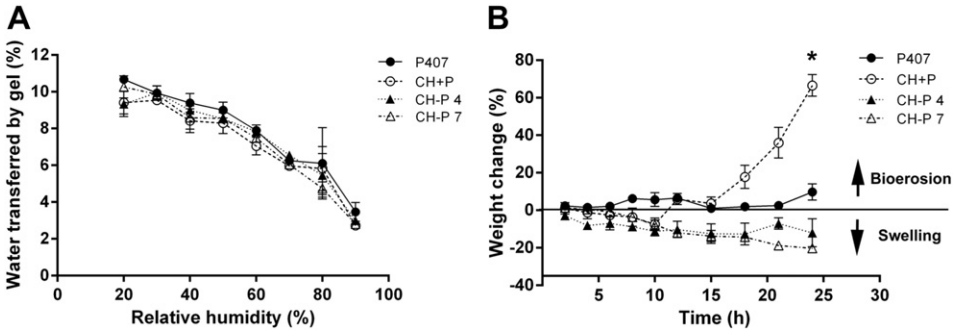

Fig. 5. Irradiated hydrogels modulate RH environment and possess the ability to absorb human sera. A) Water transfer capability of different hydrogels at various relative humidities (RH). Data are presented as mean ± Standard Error of the Mean (S.E.M.). Significant differences with one-way Analysis of Variance (ANOVA) followed by Tukey's test as follows post hoc: at 60% RH (CH+P vs. P407, $p = 0.0373$); at 70% RH (CH-P 4 vs. CH+P, $p = 0.0101$, and CH-P 7 vs. CH-P 4, $p = 0.0224$). B) Bioerosion or swelling behavior of the different hydrogels as a modification produced by gamma irradiation. Significant differences with Tukey's post hoc test focused at 24 h as follows: CH+P vs. P407, $p < 0.0001$; CH-P 4 vs. P407, $p = 0.0029$; CH-P 7 vs. P407, $p = 0.0005$; CH-P 4 vs. CH+P, $p < 0.0001$, and CH-P 7 vs. CH+P, $p < 0.0001$).

on *Candida albicans*, but CH+P, as well as CH-P 4, did (Table 2), possibly by means of the additional factor of acid pH, a medium acid that aids in counteracting bacterial growth. The importance of protonated CH amino groups was evidenced by the antifungal effect observed when *Candida albicans* cultures were treated with CH+P and CH-P 4, but this was absent with the CH-P 7 hydrogel. The increased antifungal activity of CH-P 4 compared with that of the other formulas was attributed to structural changes due to gamma radiation, in that only CH-P 4 reached the highest degree of inhibition. These results indicate that the different compounds evaluated act selectively against a broad spectrum of pathogens and that application of irradiated hydrogels on infected wounds could be highly

Table 2
Irradiated hydrogels exhibit antimicrobial, and antifungal properties in a pH-dependent manner. Halos of inhibition produced by different materials-of-interest against different microorganisms. Data are presented as means.

Microorganism	Halos of inhibition (mm)					
	Negative control	P407	CH	CH+P	CH-P 4	CH-P 7
Escherichia coli (ATCC25922)	0	0	9	10	10	10
Staphylococcus aureus (ATCC29213)	0	0	10	11	10	10
Pseudomonas aeruginosa (clinical isolate)	0	0	8	10	10	11
Candida albicans (clinical isolate)	0	0	11	9	11	0

One-way Analysis of Variance (ANOVA), followed by Tukey test for halos of inhibition was carry out. For *E. coli*, *S. aureus*, and *P. seruginosa* the measurements of halos of inhibition for all hydrogels composed of CH were statistically significant ($p < 0.05$) compared with P407 and control. For *C. albicans*, the measurements of halos of inhibition were statistically significant ($p > 0.05$) compared to CH-P 7, P407 and control.

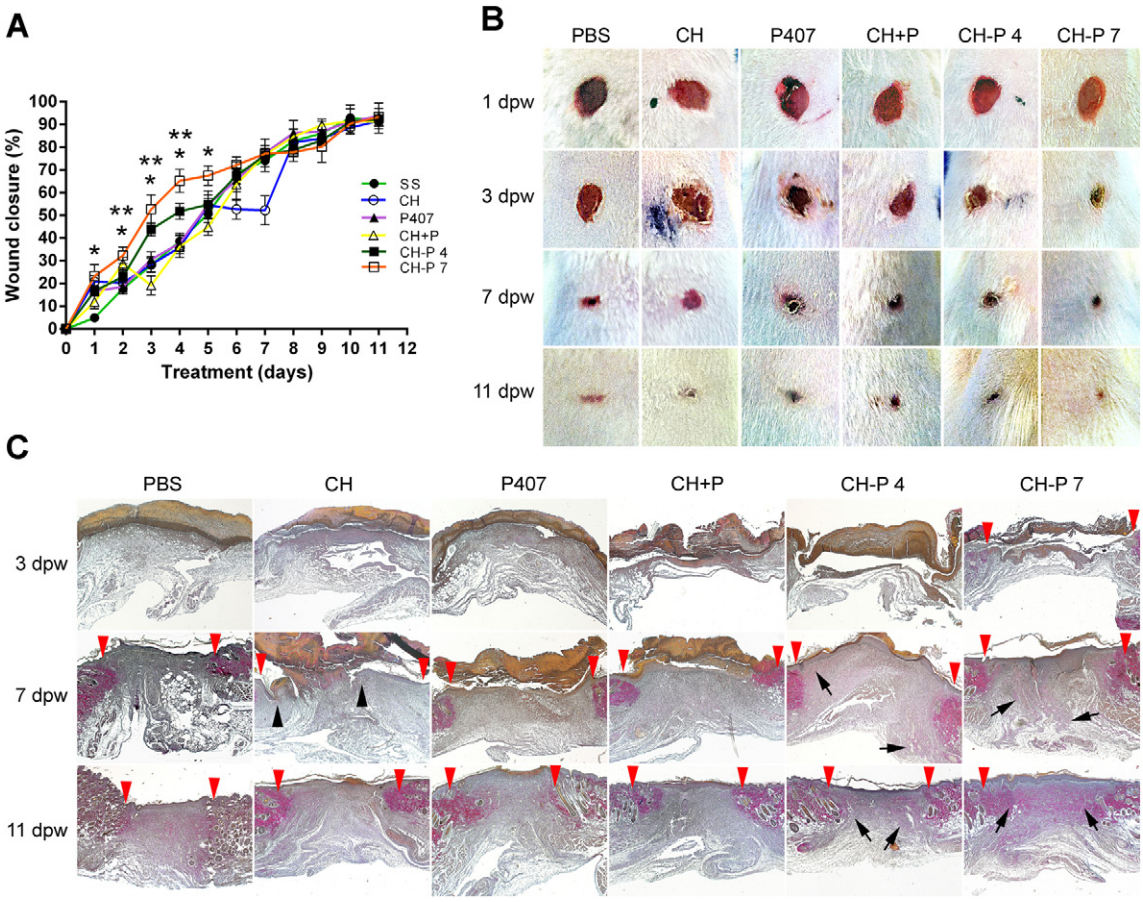

Fig. 6. Wound treated with irradiated hydrogels showed an increase in wound closure during the first days of repair. A) The excisional wound-closure percentage in the dorsal region of male CD1 mice during different treatment days with hydrogels is depicted. Statistical analyses were performed using JMP software (SAS, USA), and the statistical significance of differences among groups for wound- closure area was determined by one-way Analysis of Variance (ANOVA), followed by the Tukey test. Data are presented as mean ± Standard Error of the Mean (S.E.M.) of the wound-closure area in a percentage, with $p > 0.05$ considered significant. B) Macroscopic composition of wounds with different treatments over time; a slight decrease in wound size was observed with CH-P 7. C) Herovici staining in histological sections of wounds treated with the different compounds. Red arrowheads indicate original wound edges, black arrowheads in wounds of 7 days treated with CH indicate re-epithelialized edges, while arrows denote collagen deposition observed in magenta. Collagen deposition was more evident in wounds treated with CH-P 7.

convenient because infection in an injury is a very common condition encountered in clinical practice.

3.2.4. Evaluation of wound closure

To evaluate the effect of CH, P407, CH+P, CH-P 4, and CH-P 7 on wound closure, a cutaneous excisional wound-healing model was employed. Notably, wounds treated with CH exhibited a closure delay. This contrasted with Ribeiro, et al. studies [3], in which the authors found a decrease in wound size during day 1 of repair with CH treatment [3]. In that work, the authors observed that, due to the saturation of P407, CH was dissolved only at a low concentration (0.75 vs. 4% w/v); additionally, deacetylation degree and MW was lower, and this may produce a different response in wound repair. With respect to P407, we did not find changes in closure rate, in contrast with what was reported by Kant et al. The latter is not clear but the wound model could exert an influence on wound response [7].

The irradiated hydrogels greatly stimulated early wound closure when compared with other treatments (Fig. 6A and B). The interaction with different relative humidities and bioerosion/swelling tests described previously suggest that irradiated hydrogels maintain the wound wet and control exudative wound fluid, thereby contributing to the acceleration of wound closure during the first days of healing. After the first week of daily treatment, CH-P 4 and CH-P 7 ceased to close the wound, demonstrating no difference with other treatments, including PBS (Fig. 6A and B). The maximal effect recorded was at day 11, where all of the animals exhibited approximately the same 93% of wound closure (Fig. 6A). Unexpectedly, wound closure was inhibited progressively after day 7 in wounds treated with irradiated hydrogels. Due to these results, we propose that treatment of wounds by CH-P 7 could be suspended after week 1 of application.

3.2.5. Histological and immunofluorescence analyses

To analyze whether the irradiated hydrogels and the remaining polymers affected the wound-healing process, histological (Fig. 6C) and immunofluorescent (Fig. 7) assays were carried out during the inflammatory, proliferative, and at the beginning of tissue-remodeling phases in wounds treated with the polymers. At day 3 post-wound (dpw), it was found that wounds treated with CH+P, CH-P 4, and CH-P 7 exhibited new ECM synthesis, which was deposited in sparse and loose parallel fibers, the latter contrary to other treatments, which demonstrated abundant and compact ECM (Fig. 6C). This organization and shortage of provisional matrix might facilitate fibroblast migration and proliferation to the wound area, contributing to the acceleration of wound closure [33].

At that time, the scab observed in tissues treated with CH-7 was thinner and was separated from the wound bed, in contrast with those treated with other formulas. This effect was particularly notable at day 7 of treatment, reflecting an acceleration of wound healing with the CH-P 7 treatment (Fig. 6C). At 7 dpw, epithelialization and granulation tissue was observed in all of the animals evaluated; however, Herovici staining indicated that wounds treated with CH-P 4 and CH-P 7 exhibited higher deposition of type I collagen in the wounded area

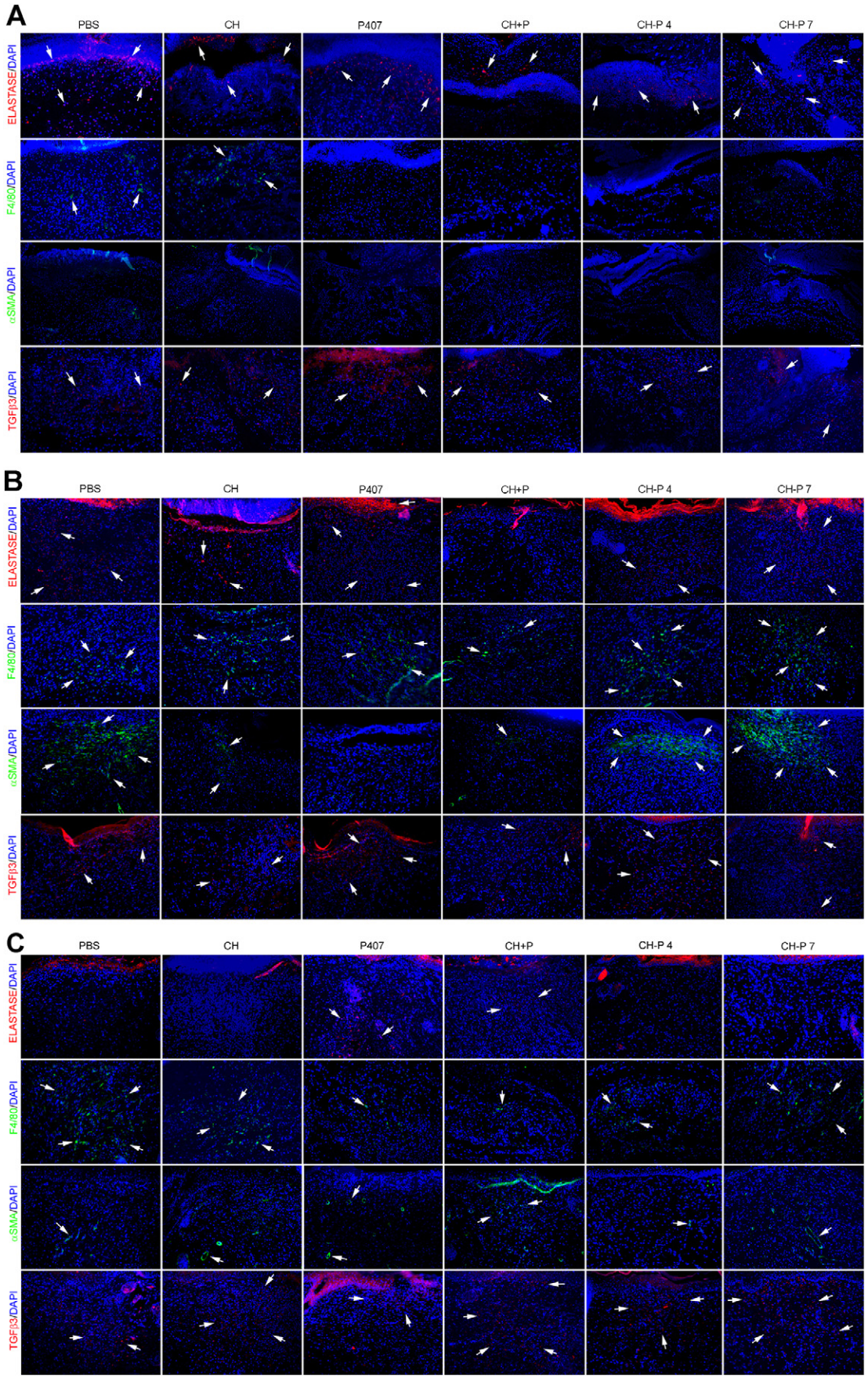
A
PBS
CH
P407
CH+P
CH-P 4
CH-P 7
ELASTASE/DAPI
F4/80/DAPI
αSMA/DAPI
TGFβ3/DAPI
B
PBS
CH
P407
CH+P
CH-P 4
CH-P 7
ELASTASE/DAPI
F4/80/DAPI
αSMA/DAPI
TGFβ3/DAPI
C
PBS
CH
P407
CH+P
CH-P 4
CH-P 7
ELASTASE/DAPI
F4/80/DAPI
αSMA/DAPI
TGFβ3/DAPI

than other treatments (Fig. 6C). It is noteworthy that wounds treated with CH exhibited an important delay in re-epithelialization, reflecting a decrease in wound closure during the first 7 dpw, which is in accordance with wound-closure kinetics, physical appearance, and histomorphology (Figs. 6A–6C). The increase of type I collagen deposition in CH-P 7-treated wounds was evident at 11 dpw, when the tissue-remodeling phase had initiated, indicating an acceleration of new tissue maturation and scar formation through this treatment.

Although it has been reported that the primary role of inflammation is to prevent bacterial infection, deregulation of the inflammatory response may result in chronic wound development or may contribute to hypertrophic scar-tissue formation [34–35]. Thus, infiltration of the main inflammatory cells, neutrophils, and macrophages in wounds treated with the different polymers was evaluated. Wounds treated with irradiated compounds, as well as wounds treated with CH+P and CH, demonstrated a slight decrease of neutrophils, visualized by the antineutrophil elastase antibody, in comparison with wounds treated with P407 and PBS at 3 dpw (Fig. 7A). Macrophages were detected at this time point only in wounds with PBS and CH (Fig. 7B). At 7 dpw, fewer neutrophils were observed in wounds treated with CH+P and irradiated compounds in comparison with the remaining treatments, and a slight increase of macrophages was observed in wounds with CH-P 7 (Fig. 7B). Also, at this time point, a persistence of neutrophils in wounds treated with CH alone was observed (Fig. 7B). At 11 dpw, neutrophils were observed solely in wounds with CH+P and P407, and macrophages were higher in wounds treated with CH and PBS, compared with the remainder of the treatments (Fig. 7C). The lower presence of neutrophils observed at 3 dpw in wounds treated with all compounds containing CH suggests that this polymer could act as an inflammation modulator only during the initial days of healing. In fact, CH powder and CH acetate bandage applied to full-thickness wounds resulted in a diminished number of inflammatory cells [36–37]. However, it was observed that wounds treated with CH alone exhibited a persistent presence of neutrophils at 7 dpw and macrophages at 11 dpw, unlike the other treatments (Fig. 7B and C). Interestingly, it has been reported that one effect of cotton fiber-type CH on open skin wounds comprised severe infiltration of polymorphonuclear cells [38]. In addition, a nano-titanium oxide-chitosan composite with artificial collagen skin slightly diminished InterLeukin (IL)-6 levels in the animal's serum, suggesting that CH modulates the immune response through IL-6, which could act as an inflammatory or anti-inflammatory factor [39]. Our results suggest that this form of CH (75–85% deacetylated) acts at two levels: it diminishes the neutrophil infiltrate only during the first days of wound repair and inhibits the resolution of inflammatory infiltrate in the subsequent stages of wound repair. The sustained neutrophil levels after 3 dpw and at 7 dpw could explain the delay in wound closure observed in mice treated with CH. It has been reported that P407 can also induce leukocyte infiltration [7]. This is consistent with the presence of neutrophils at 3, 5, and 11 dpw in wounds treated with P407. These observations indicate that materials could contribute to inflammation regulation due to the presence of CH and P407.

In addition to their inflammatory role, macrophages are important sources of growth factors, including TGFβ1, which, among others, induce myofibroblast differentiation evidenced by α-SMA expression. Myofibroblasts are responsible for wound contraction and collagen synthesis, and they are present at higher proportions during fibroplasia [40–41,35]. At 7 dpw, an increase in the macrophage and myofibroblast proportion was visualized by F4/80 and α-SMA expression, respectively, in tissues treated with CH-P 7 (Fig. 7B). These results suggested that early activation of fibroblasts could contribute to the acceleration of wound closure during the first days by contraction and to the promotion of scar-tissue maturation in wounds. High levels of TGFβ3 expression have been associated with scar-free wound resolution and with the reduction of hypertrophic scars [42–43]. To test whether high-quality resolution could be acquired during treatment with irradiated hydrogels, we searched TGFβ3 expression as a marker of scar-free healing in such wounds. We did not find changes in TGFβ3 levels in any treatment, indicating that CH-P 7 does not induced high-quality wound resolution.

4. Conclusion

In this work, CH-P 4 and CH-P 7 were obtained by gamma irradiation through a fast, economical, and environmentally friendly procedure, with biodegradable and biocompatible materials. Thermo-reversibility and gelation properties at a low temperature allow for easy application to the wound, while the ability to swell in the presence of human serum permits the control of excessive exudate for skin-wound application. Also, the new material maintains the antimicrobial/antifungal effect by means of acid pH and/or by CH properties. Additionally, studies in vivo indicated that CH-P 7 possesses highest wound-closure rate during week 1 in mice. This observation correlates with an increase of macrophages, α-SMA expression, and collagen synthesis, resulting in a more mature repair. All of these beneficial properties confer the ability on this novel material to address wound-closure with different mechanisms of action, both physical and biological. Therefore, its usefulness may be of high potential, either alone or in combination with active pharmaceutical ingredients.

Conflict of interest

The authors declare no conflict of interest. This work is consistent with the Journal's guidelines for ethical publication.

References

[1] M. Dash, F. Chiellini, R.M. Ottenbrite, E. Chiellini, Chitosan—a versatile semi-synthetic polymer in biomedical applications, Prog. Polym. Sci. 36 (2011) 981–1014.
[2] M. Cheng, J. Deng, F. Yang, Y. Gong, N. Zhao, X. Zhang, Study on physical properties and nerve cell affinity of composite films from chitosan and gelatin solutions, Biomaterials 24 (2003) 2871–2880.
[3] M.P. Ribeiro, A. Espiga, D. Silva, P. Baptista, J. Henriques, C. Ferreira, J.C. Silva, J.P. Borges, E. Pires, P. Chaves, I.J. Correia, Development of a new chitosan hydrogel for wound dressing, Wound Repair Regen. 17 (2009) 817–824.
[4] S. Anjum, A. Arora, M.S. Alam, B. Gupta, Development of antimicrobial and scar preventive chitosan hydrogel wound dressings, Int. J. Pharm. 508 (2016) 92–101.
[5] L. Klouda, A.G. Mikos, Thermoresponsive hydrogels in biomedical applications, Eur. J. Pharm. Biopharm. 68 (2008) 34–45.
[6] D.D. Ramya, P. Sandhya, B.N. Vedha, Poloxamer: a novel functional molecular for drug delivery and gene therapy, J. Pharm. Sci. Res. 5 (2013) 159–165.
[7] V. Kant, A. Gopal, D. Kumar, A. Gopalkrishnan, N.N. Pathak, N.P. Kurade, S.K. Tandan, D. Kumar, Topical pluronic F-127 gel application enhances cutaneous wound healing in rats, Acta Histochem. 116 (2014) 5–13.
[8] A.B. Lugao, S.M. Malmonge, Use of radiation in the production of hydrogels, Nucl. Inst. Methods Phys. Res. B 185 (2001) 37–42.
[9] Z. Ajji, G. Mirjalili, A. Alkhatab, H. Dada, Use of electron beam for the production of hydrogel dressings, Radiat. Phys. Chem. 77 (2008) 200–202.
[10] G. Leyva-Gómez, E. Lima, G. Krötzsch, R. Pacheco-Marín, N. Rodríguez-Fuentes, D. Quintanar-Guerrero, E. Krötzsch, Physicochemical and functional characterization of the collagen-polyvinylpyrrolidone copolymer, J. Phys. Chem. B 118 (2014) 9272–9283.
[11] X. Huang, Y. Zhang, X. Zhang, L. Xu, X. Chen, S. Wei, Influence of radiation crosslinked carboxymethyl-chitosan/gelatin hydrogel on cutaneous wound healing, Mater. Sci. Eng. C Mater. Biol. Appl. 33 (2013) 4816–4824.
[12] Y.S. Choi, S.R. Hong, Y.M. Lee, K.W. Song, M.H. Park, Y.S. Nam, Study on gelatin-containing artificial skin: I. Preparation and characteristics of novel gelatin-alginate sponge, Biomaterials 20 (1999) 409–417.
[13] L. Zhao, H. Mitomo, M. Zhai, F. Yoshii, N. Nagasawa, T. Kume, Synthesis of antibacterial PVA/CM-chitosan blend hydrogels with electron beam irradiation, Carbohydr. Polym. 53 (2003) 439–446.
[14] K.M. El-Salmawi, Gamma radiation-induced crosslinked PVA/chitosan blends for wound dressing, J. Macromol. Sci. A 44 (2007) 541–545.

Fig. 7. Wounds treated with irradiated hydrogels showed an increase in F4/80 and α-SMA expression that correlates with the accelerated presence of collagen matrix. Immunofluorescence to detect neutrophil elastase, F4/80 (macrophages), α-SMA, and TGFβ3 in wounds treated daily with the different compounds. Analysis was performed on days 3 (A), 7 (B), and 11 (C) post-wound (dpw). Arrows indicate the expression area of α-SMA or cells positive for neutrophil elastase, F4/80, or TGFβ3.

[15] X. Yang, K. Yang, S. Wu, X. Chen, F. Yu, J. Li, M. Maa, Z. Zhua, Cytotoxicity and wound healing properties of PVA/ws chitosan/glycerol hydrogels made by irradiation followed by freeze–thawing, Radiat. Phys. Chem. 79 (2010) 606–611.
[16] M.T. Razzak, D. Darmawan, S. Zainuddin, Irradiation of polyvinyl alcohol and polyvinyl pyrrolidone blended hydrogel for wound dressing, Radiat. Phys. Chem. 62 (2001) 107–113.
[17] J. Dutta, Synthesis and characterization of γ-irradiated PVA/PEG/CaCl2 hydrogel for wound dressing, Am. J. Chem. 2 (2012) 6–11.
[18] E.A. Kamoun, X. Chen, S. Mohamed, M.S.E. Mohy, E.S. Kenawy, Crosslinked poly(vinyl alcohol) hydrogels for wound dressing applications: a review of remarkably blended polymers, Arab. J. Chem. 8 (2015) 1–14.
[19] L. Mayol, F. Quaglia, A. Borzacchiello, L. Ambrosio, M.I. La Rotonda, A novel poloxamers/hyaluronic acid in situ forming hydrogel for drug delivery: rheological, mucoadhesive and in vitro release properties, Eur. J. Pharm. Biopharm. 70 (2008) 199–206.
[20] S. Kumar, V. Deepak, M. Kumari, P.K. Dutta, Antibacterial activity of diisocyanate-modified chitosan for biomedical applications, Int. J. Biol. Macromol. 84 (2016) 349–353.
[21] T. Du, Z. Chen, H. Li, X. Tang, Z. Li, J. Guan, C. Liu, Z. Du, J. Wu, Modification of collagen-chitosan matrix by the natural crosslinker alginate dialdehyde, Int. J. Biol. Macromol. 82 (2016) 580–588.
[22] Y.W. Cho, J. Jang, C.R. Park, S.W. Ko, Preparation and solubility in acid and water of partially deacetylated chitins, Biomacromolecules 1 (2000) 609–614.
[23] D. Attwood, Z. Zhou, C. Booth, Poly(ethylene oxide) based copolymers: solubilisation capacity and gelation, Expert Opin. Drug Deliv. 4 (2007) 533–546.
[24] I.M. El-Bagory, M.A. Bayomi, G.M. Mahrous, F.K. Alanazi, I.A. Alsarra, Effect of gamma irradiation on pluronic gels for ocular delivery of ciprofloxacin: in vitro evaluation, Aust. J. Basic Appl. Sci. 4 (2010) 4490–4498.
[25] E. Caló, V.V. Khutoryanskiy, Biomedical applications of hydrogels: a review of patents and commercial products, Eur. Polym. J. 65 (2015) 252–267.
[26] K. Vowden, P. Vowden, Wound dressings: principles and practice, Surgery 32 (2014) 462–467.
[27] A. Tarig, H. Newton, Wound dressings: principles and practice, Surgery 29 (2011) 491–495.
[28] C. Ghobril, M.W. Grinstaff, The chemistry and engineering of polymeric hydrogel adhesives for wound closure: a tutorial, Chem. Soc. Rev. 44 (2015) 1820–1835.
[29] B. Gupta, R. Agarwal, M. Alam, Hydrogels for wound healing applications, in: S. Rimmer (Ed.), Biomedical Hydrogels, Biochemistry, Manufacture and Medical Applications, Woodhead Publishing, Oxford 2011, pp. 184–227.
[30] S.C. Park, J.P. Nam, J.H. Kim, Y.M. Kim, J.W. Nah, M.K. Jang, Antimicrobial action of water-soluble β-chitosan against clinical multi-drug resistant bacteria, Int. J. Mol. Sci. 16 (2015) 7995–8007.
[31] Y. Park, M.H. Kim, S.C. Park, H. Cheong, M.K. Jang, J.W. Nah, K.S. Hahm, Investigation of the antifungal activity and mechanism of action of LMWS-chitosan, J. Microbiol. Biotechnol. 18 (2008) 1729–1734.
[32] M.S. Benhabiles, R. Salah, H. Lounici, N. Drouiche, M.F.A. Goosen, N. Mameri, Antibacterial activity of chitin, chitosan and its oligomers prepared from shrimp shell waste, Food Hydrocoll. 29 (2012) 48–56.
[33] Z.J. Rutnam, T.N. Wight, B.B. Yang, miRNAs regulate expression and function of extracellular matrix molecules, Matrix Biol. 32 (2013) 74–85.
[34] G.G. Walmsley, Z.N. Maan, V.W. Wong, D. Duscher, M.S. Hu, E.R. Zielins, T. Wearda, E. Muhonen, A. McArdle, R. Tevlin, D.A. Atashroo, K. Senarath-Yapa, H.P. Lorenz, G.C. Gurtner, M.T. Longaker, Scarless wound healing: chasing the holy grail, Plast. Reconstr. Surg. 135 (2015) 907–917.
[35] S.A. Eming, T. Krieg, J.M. Davidson, Inflammation in wound repair: molecular and cellular mechanisms, J. Invest. Biol. 127 (2007) 514–525.
[36] Y. Okamoto, K. Shibazaki, S. Minami, A. Matsuhashi, S. Tanioka, Y. Shigemasa, Evaluation of chitin and chitosan on open wound healing in dogs, J. Vet. Med. Sci. 57 (1995) 851–854.
[37] M. Burkatovskaya, A.P. Castano, T.N. Demidova-Rice, G.P. Tegos, M.R. Hamblin, Effect of chitosan acetate bandage on wound healing in infected and noninfected wounds in mice, Wound Repair Regen. 16 (2008) 425–431.
[38] H. Ueno, H. Yamada, I. Tanaka, N. Kaba, M. Matsuura, M. Okumura, T. Kadosawa, T. Fujinaga, Accelerating effects of chitosan for healing at early phase of experimental open wound in dogs, Biomaterials 20 (1999) 1407–1414.
[39] C.C. Peng, M.H. Yang, W.T. Chiu, C.H. Chiu, C.S. Yang, Y.W. Chen, K.C. Chen, R.Y. Peng, Composite nano-titanium oxide-chitosan artificial skin exhibits strong wound-healing effect-an approach with anti-inflammatory and bactericidal kinetics, Macromol. Biosci. 8 (2008) 316–327.
[40] S. Werner, R. Grose, Regulation of wound healing by growth factors and cytokines, Physiol. Rev. 83 (2003) 835–870.
[41] R.A. Evans, Y.C. Tian, R. Steadman, A.O. Phillips, TGF-beta1-mediated fibroblast-myofibroblast terminal differentiation-the role of Smad proteins, Exp. Cell Res. 282 (2003) 90–100.
[42] D. Honardoust, M. Varkey, Y. Marcoux, H.A. Shankowsky, E.E. Tredget, Reduced decorin, fibromodulin, and transforming growth factor-β3 in deep dermis leads to hypertrophic scarring, J. Burn Care Res. 33 (2012) 218–227.
[43] M. Shah, D.M. Foreman, M.W. Ferguson, Neutralisation of TGF-beta 1 and TGF-beta 2 or exogenous addition of TGF-beta 3 to cutaneous rat wounds reduces scarring, J. Cell Sci. 108 (1995) 985–1002.